中國機械工程學刊第三十九卷第六期第 609~618 頁(民國一百零七年)
Journal of the Chinese Society of Mechanical Engineers, Vol.39, No.6, pp 609~618 (2018)

Numerical Treatment of Parametric Gradient Problems in Source Term by New Difference Methods

Tzong-Hann Shieh*,**, Meng-Rong Li***, Yu-Tso Li**,****and Yung-Ting Chen**

Keywords： gradient method, Euler equations, numerical oscillation, shock capturing.

ABSTRACT

In this paper, we expand the energy equation of unsteady Euler equations as the form of mixture gas and carry out the numerical resolution through the FVM to discuss the nonphysical oscillations near the contact discontinuity interface and shock wave. We resolve the equations by using the AUSMDV Riemann solver with different flux limiters, the FVM and the second-order with two-step discrete-time stepping method. For the source term in the investigated Euler equations with multi-species, we discuss the facing problem of for the numerical treatment of gradient in different type and test the non-physical oscillation problem by establishing a new applied method of gradient control.

INTRODUCTION

The unsteady high enthalpy flow field causes the flow field problems in the experiment of shock tube, particularly in the moving process of contact surface between the different gases in the shock tube. In other words, when we carry out the numerical simulation by using approximate the Riemann solver method, it will produce the non-physical oscillations near the contact discontinuity and shock wave.

Paper Received December, 2017. Revised October, 2018. Accepted November, 2018. Author for Correspondence: Yu-Tso Li

* *Department of Aerospace and Systems Engineering, Feng Chia University. 100, Wenhwa Rd., Seatwen, Taichung, Taiwan.*

** *Ph.D. Program of Mechanical and Aeronautical Engineering, Feng Chia University. 100, Wenhwa Rd., Seatwen, Taichung, Taiwan.*

*** *Department of Mathematical Sciences, National Chengchi University. 64, Sec. 2, ZhiNan Rd., Wenshan District, Taipei, Taiwan.*

**** *Department of Mechanical Engineering, Minghsin University of Science and Technology. No.1, Xinxing Rd., Xinfeng Hsinchu 30401, Taiwan*

In 1981, Jameson et al. (1981) has proposed a result that the rapid change of entropy and the occurrence of eddy is unable to be considered by approximation neglect way when exceeding the range of transonic. Therefore, for the numerical simulation problem of supersonic and hypersonic flow field, savants have made deep researches over the last three decades.

For the flux vector questions of compressible Euler equations, van Leer (1984) discussed the type of shock wave under the steady state between the two regions based on the first order upwind scheme in 1984. In addition, for the problems of hypersonic un-differential point and stagnation point, that we treat this kind question with the type of split fluxes has the equivalent advantage according to the form developed by Steger and Warming.

The process of directly numerical solver will produce some difficulty for the Riemann problem of unsteady hypersonic flow field due to the non-linear situation when the conservation equations of flow status is solved by numerical solver. Thus, in the 1950s, Godunov (1950) proffered an opinion at the earliest that we can obtain the accurately exact solution by using the information of the previous time point containing the conservation frame to deal with the discretization conservation equation of single ideal gas. Additionally, van Leer developed the MUSCL numerical reconstruction method and established the TVD scheme so that the process of numerical computing gets a consequence of high order accuracy in 1979. Moreover, in 1994, Wada and Liou (1994) offered the approximation Riemann solver method of split fluxes scheme AUSMDV that is an improved upwind split scheme based on AUSM principle. Through this computing method on the numerical computing code of high resolution, it will avoid the violent oscillations in some regions, especially the positions of shock wave and contact discontinuity interface.

To improve the above non-physical oscillation

problem near the contact discontinuity interface and shock wave, we expand the energy equation of Euler equations as the type of ideal mixture gas through the AUSMDV numerical flux scheme, see Ton (1996), and adding the different flux limiters as well as gradient control. For the pressure and velocity gradient of source term, we propose various gradient computation ways to mend the approximation error problem caused by the energy and pressure parameter of source term near the moving shock and contact discontinuity interface. For the pressure and velocity gradient of source term, we established the new method of gradient control to test whether it can make progress in the non-physical numerical oscillation problem.

MODELLING

Conservation Equations with Gas Mixture

In this study, we consider 1D-Euler equations with gas mixture model in general form,

$$\frac{\partial}{\partial t}\int_V U dx + \int_{\partial V} F dA = \int_V Q dx, \qquad (1)$$

where V stands for volume, U is the vector relation of conservation variables, ∂V represents surface, F is frictionless flux vector and Q depicts the vector parameter of source terms, see Shieh and Li (2009). Those vector parameters could be defined as

$$\mathrm{U} = \left[\rho_i, \rho u, \rho_i E_i, \rho E\right],\ \mathrm{F} = \left[\rho_i u, \rho u^2 + P, \rho_i E_i u, \rho E u + P u\right],$$

$$Q = \left[0, 0, -\left(Y_i u \frac{\partial}{\partial x} P + \frac{P_i P}{\gamma_i \sum_{j=1}^{ns} \frac{P_j}{\gamma_j}} \frac{\partial}{\partial x} u\right), 0\right].$$

Based on gas mixture, the third vector describes the additional energy source term which Ton (1996) expand it. Therefore, the different two densities ρ_1 and ρ_2 just get the energy of other species from the total energy and produce an extra individual energy $\rho_1 E_1$. In the above vector matrices, mixing specific heat ratio γ is simplified as

$$\gamma = 1 + \left[\sum_{i=1}^{ns}\left(Y_i / W_i\right) \Big/ \sum_{i=1}^{ns}\left(Y_i / \left(W_i\left(\gamma_i - 1\right)\right)\right)\right].$$

Moreover, the thermodynamic function among the individual pressure P_i, energy E_i and specific heat ratio γ_i is shown as $P_i = (\gamma_i - 1)(\rho_i E_i - (1/2)\rho_i u^2)$.

Pressure Gradient

For the pressure gradient problem of source term in the expanding energy equation; however, we try to deal with this problem using some distinct models. We expand the distinct pressure P_i through the following Taylor series with the third order differential term

$$\frac{\partial \mathrm{P(x,t)}}{\partial \mathrm{x}} = \frac{\partial^2 P}{\partial x^2}(\Delta x) + \frac{1}{2}\frac{\partial^3 P}{\partial x^3}(\Delta x)^2 + O((\Delta x)^3). \qquad (2)$$

In order to treat the problems of pressure gradient, we separately estimate the difference of density ρ_i, temperature T_i and gas constant R_i by the equation of state, $\nabla \mathrm{P} = \nabla(\rho \mathrm{RT})$, in two ways. In the first way, we consider the expression the pressure gradient is expressed by $\nabla P = R\nabla(\rho T)$, where the gas constant is invariable. In the second, we consider the extra term $\rho T \nabla R$ with the changing gas constant $R \neq$ constant. In this way, we apply the expression of pressure gradient by $\nabla P = R\nabla(\rho T) + \rho \mathrm{T} \nabla \mathrm{R}$. Moreover, we compute the pressure gradient with energy E and specific heat ratio γ, $\nabla \mathrm{P} = \nabla(\gamma\text{-}1)(\rho \mathrm{E} - (1/2)\rho u^2)$. Discrepancy compared with the equation, $\mathrm{P_i} = \nabla(\gamma_i\text{-}1)(\rho_i \mathrm{E_i} - (1/2)\rho_i u^2)$ is that we do discretization before performing the individual difference in this form.

NUMERICAL METHOD

Finite Volume Method

By the discretization of equations (1), we classify the computational domain to the distinct control volume *K*, where the boundary of individual computing cells could be defined by mesh border. We transform the difference equation into an algebraic equation by integrating along the computing cells. The equations (1) using closed volume between Δt and Δx. Now, for the computing cell boundary, we again consider the form of conservation equations as

$$\frac{\partial}{\partial t}\int_K U(x,t)dx + \oint_{\partial K} F(x,t)dA = \int_K Q(x,t)dx.$$

The variable ϕ_K is defined by

$$\phi_K(t) := \int_K Q(x,t)dx - \oint_{\partial K} F(x,t)dA.$$

Through the flux calculation in AUSMDV Riemann solver and the discretization of source term $Q(x,t)$, the individual control volume *K* is defined by the mean value *U* of every grid. For 1D space discretization, we can get a discretized form of first order time stepping by

$$\Delta \overline{U}_K = \overline{U}_K(t_2) - \overline{U}_K(t_1),$$

$$\Delta \overline{U}_K(x,t_2) = \overline{U}_K(x,t_1) + \frac{\Delta t}{\Delta x}\phi_K(x,t_s).$$

Through the process of temporal iterations, we solve the variables of temporal discretization in every volume mesh after the previous temporal and space discretization.

Time Stepping Procedure

In the presenting study, the explicit method is applied to deal with the time discretization of Eqs. (1). The restriction of stepping is denoted by v for the CFL number, where the numerical domain of dependence temporal must be lie in the physical domain,

and the steps of temporal discretization is combined with the so-called CFL stability condition by a new type $v \equiv v_{\max}(\Delta t/\Delta x)$, where Δx and $v_{\max}$ are the 1-D control volume and the maximum propagation velocity in the calculating grid respectively. The computation process is stable in the range of $0 \le v < 1$, and the CFL number is contained better in the range near 1.

For the time stepping procedure, we recall the equation (4) to obtain the following explicit two-steps second-order Runge-Kutta method with

$$U_k(x,t_2) \approx U_K(x,t_1) + \frac{1}{2}\frac{\Delta t}{\Delta x}\phi(U_K(x,t_1)) + \frac{1}{2}\frac{\Delta t}{\Delta x}\phi\left[U_K(x,t_1) + \frac{\Delta t}{\Delta x}\phi(U_K(x,t_1)) + \frac{1}{2!}\frac{(\Delta t^2)}{\Delta x}\phi^2(U_K(x,t_1))\right] \quad (5)$$

Numerical Reconstruction

The slope limiter on the both sides of grid was implemented in the applied approximation method in order to acquire the high accurate consequences. In this study, we treat the high gradient phenomenon through first order TVD mode under the following definition of $U(x,t)$ on the grid in some local extreme domain,

$$\mathrm{TV[U(,t)]} = \sup_{(\text{over all grid points } x_i)} \sum_{i=-\infty}^{\infty} \left|U(x_{i+1},t) - U(x_i,t)\right| .$$

The numerical treatment TVD is expressed by $V[U(,t_{i+1})] \le TV[U(,t_i)]$, but using the second order manner to keep the precision in the smooth domain. Additionally, the limiter function is inferred from the restriction factor φ based on the single-side gradient of neighbor grid, and these functions construct based on the minmod limiter. For this reason, two high order limiters will be applied in this case.

First, we obtain the so-called superbee limiter that is based on the region ratio r as

$$\varphi_{SB}(r) = \max\{0, \min\{2r,1\}, \min\{r,2\}\} .$$

For the second scheme, we apply the van Leer limiter with a form $\varphi_{vL}(r) = r + |r|/1 + |r|$, where the negative of r vanishes, and the positive of r keeps the smooth state as well as continuity at $r = 0$. In addition, for the fourth-order tests, we added the Čada limiter (2009), and adopted the following compression form with $\Phi(\mathrm{r},\alpha,\beta,\gamma) = (\mathrm{r},0.5,2,1.6)$

$$\varphi_{comp}(r) = \max\left\{0, \min\left\{\frac{2+r}{3}, \max\left[-0.5r, \min\left(2r, \frac{2+r}{3}, 1.6\right)\right]\right\}, \min\{2r,1\}\right\} \quad (6)$$

Moreover, the AUSMDV numerical flux function is used in this study, see e.g. Liou and Steffen (1996), van Leer (2006), Wada and Liou (1994) and Xu et al. (1994). They carried out a series of modifications and suggested reducing the numerical dissipation problem on the contact discontinuity position, and set up a combined mixture momentum flux $(\rho \mathrm{u})_{1/2}$ as

$$(\rho \mathrm{u}^2)_{1/2} = ((1/2)+s)(\rho u^2)_{AUSMV} - ((1/2)-s)(\rho u^2)_{AUSMD},$$

where s is a switching function of pressure gradient as

$$s = (1/2)\min(1, K(|P_L - P_R|/\min(P_L P_R))).$$

In this form, the weight of AUSMV is more used to maintain the capability of catching the shock wave with the constant $K = 10$.

Discretization of ∇P in Source Term

In order to reduce the error generated by the gradient calculating, we applied different orders and gradient calculating models with various difference types through the following Taylor expansion of 1D gradient of parameter f

$$\frac{\partial}{\partial x} f = \frac{\partial f}{\partial x} + \frac{\partial^2 f}{\Delta x^2}(\Delta x) + \frac{1}{2}\frac{\partial^3 f}{\partial x^3}(\Delta x)^2 + O((\Delta x^2)).$$

Approximate methods

For the parametric gradient, the diverse difference kinds were applied in the numerical calculation. In this way, we define $f^n(x,t) := f(x,t+n\Delta t)$ and $f_i(x,t) := f(x+n\Delta x,t)$. For the first-order derivative f_x, we applied the forward difference method, central difference method and backward difference method respectively. In the difference form of second order derivative f_{xx} which is just only considered by the central difference method. For the difference of third order derivative f_{xxx}, because of the confinement of computing node amount and boundary point, we consider the forward difference method, central difference method and backward difference method. Besides, we developed two newly difference method of third order derivative to reduce the error due to the profuse computation nodes, that is,

$$f_{xxx} = f_{i+2} - 2f_{i+1} + f_i/(\Delta x)^3 \quad (7)$$

and $f_{xxx} = f_{i+2} - 2f_{i+1} + f_i/2(\Delta x)^3$. (8)

We appoint the form (7) and (8) as N1 and N2 individually. For the difference form of fourth order derivative f_{xxxx}, we just adopted the central difference method.

Effective loop design

In the calculating process, if the node position is incorrect, it will lead to wrong of calculation. Hence, we applied the following difference mode and notion of effective loop design:

(a) Gradient based on the first order derivative

For the first order derivative, if the central or backward difference is applied to approximate, it

is easy to obtain some errors on the boundary. In addition, because of the missing values, the condition for the point is possibly neglected. For this reason, we applied the forward difference method in the first order derivative to avoid that the error may occur at the initial position.

(b) Gradient based on the second order derivative

In order to better the precision on the high order derivative calculation, we consider the form of central difference in the second order derivative. On the early test, we almost applied the combination which picking the forward difference for the first order derivative and the central difference for the second order derivative to estimate the gradient relation of second order derivative. And then, on the late test, we also try to add the switch loop dodging the position of $t=-1$ and extending the type of second order derivative after $t=1$.

(c) Gradient based on the third order derivative and mixture difference type

It needs more than 5 nodes to estimate the third order derivative. However, shock wave and contact discontinuity interface both are momentary physical characteristics for the discussed Riemann question. It will be lead to problems which are wrong estimation and acute oscillations as well as unable to calculate on the shock wave and contact discontinuity interface when the computing nodes are excessive. Hence, we employ the difference method of third order derivative with three nodes. Additionally, we try to add mixed loop; further we discuss the following issues.

(i) Fix the gradient calculation of third-order derivative, we test the different ways and types of distinct difference association.

(ii) Fix the computation of first and second order derivative, we add the difference methods of third derivative to compute the gradient according to the distinct difference type between $t=2$ and 4.

(iii) Begin at the first order derivative we add the difference of diverse order derivative in accordance with the position of the earliest node of selected difference type. Take the forward difference method for the first order derivative and the central difference method for the second and third order derivative. The initial position of central difference of second order derivative is at $t=-1$, and the central difference of third order derivative starts to compute at $t=-2$. Therefore, we add the second order derivative at $t=1$ such that the gradient computation with the second order difference begin at $t=1$. In addition, add the third order derivative at $t=2$ and the gradient will be estimated by the third order difference method after $t=2$.

For the discussed problem, we select the suitable way to compute the gradient through the above ideas of difference and loop design.

TESTING AND INITIAL CONDITION SETTING

In order to evaluate the additional energy term expanded by multispecies problem. We discuss and analyze the results of new gradient mode applied in the additional energy term through the shock tube problem of single gas. First, we discuss the merits and computing efficiency for the condition of shock tube problem with single gas as Table 2. Here, for the "shock tube problem", we adopt air, and the foundational parameters of gas separately molecular weight $W=28.97$, gas constant $R=0.287$ and specific heat ratio $\gamma=1.4$. On the other hand, for the boundary conditions of the problem, we identically set that the stepping size of the space discretization $\Delta x=0.01$, the stability factor $C_{CFL}=0.9$ and the maximal time steps equal to 20000.

The conditions of reference solution are shown as the Table 1. We adopt the minimum displacement step and the higher stability condition matching the more stable van Leer limiter as well as the second-order Runge-Kutta time stepping method in order to avoid producing the numerical oscillations and obtain an approximation accurate solution.

Table 1. The initial condition of the reference solution

	Δx	C_{CFL}	Limiter	Integration
Reference solution	0.0001	0.9	van Leer	Second-order Runge-Kutta method

Table 2. The single-gas initial condition of shock tube problem

Air	ρ_1	ρ_2	u	P	Y_1	Y_2	x
Left hand side(L)	1	0	0	1	1	0	$x<0.5$
Right hand side(R)	0.8	0	0	0.2	1	0	$x\geq 0.5$

Because we hope that the computing code has the accurate and efficient catching shock capability and the perfect calculation model is proposed effectively for the testing question, we confirm the new gradient modes. Additionally, we adopt air to test for the single gas problem, and the condition on both sides of membrane is shown as Table 2. The difference is that the time stepping stops at time $t=0.33$ and the initial position of central membrane is $x=0.5$ between this problem and the

above problem.

In order to verify the additional energy term expanded by the mixture gas problem, we also consider the two-gas condition, that is, air and helium (He). The molecular weight (W) of air is 28.97, gas constant (R) is 0.287 and specific heat ratio γ is 1.4; that of helium (He) is 4.003, 2.0769 and 1.667 separately. We identically set the boundary conditions of the problem as the above description of single-gas condition and the dual-gas condition as Table 3.

Table 3. The dual-gas initial condition of shock tube problem

Gas condition	ρ_1	ρ_2	u	P	Y_1	Y_2	x
Left hand side(L)	1	0	0	1	1	0	$x < 0.5$
Right hand side(R)	0	0.8	0	0.2	0	1	$x \geq 0.5$

For the presented diagram of regional locations, Zoom1 is the extremity position of expansion wave, Zoom2 stands for the starting area of contact discontinuity interface, Zoom3 represents the region between contact discontinuity interface and shock wave and Zoom4 shows the rear edge of shock wave. Moreover, for the ρE -related diagram, Zoom2 stands for the rear edge of expansion wave as well as Zoom3 is the region between contact discontinuity interface and shock wave.

NUMERICAL RESSULTS AND DISCUSSION

In order to treat the gradient problem, we applied the Runge-Kutta time stepping method with second order, van Leer limiter and Superbee limiter.

The Gradient Computation with Different Types under Single Gas Condition

For the gradient problem of source term in the additional equation, we carried out the gradient problem through the following two ways.

- **The gradient difference forms with different order:**
  First, we analyze and discuss that increasing order of difference whether raise the computing accuracy through fixing the difference type of distinct order.
- **Changing types of gradient difference method:**
  For the difference types of mixture loop, we analyze the problems that are numerical oscillations and failed projections on the shock wave and contact discontinuity interface by changing difference types.

Comparison of Gradient Difference Method with Distinct Order

We first discuss the results of third order derivative based on the gradient model through Taylor series. The types of difference were applied as Table 4, where the difference methods *N1* and *N2* of third order derivative were explained in detail by Eqs. (7) and (8) on the above section. In order to escape from the confusing difference type, we define the symbols as Table 5. For example, "$F^1B^2C^3$" stands for the form that the forward, backward and central difference methods are separately used in the first, second and third order derivative.

Table 4. The adopted difference methods

Derivative	Forward difference (FD)	Backward difference (BD)	Central difference (CD)	Other difference method
f_x	✓	✓	✓	
f_{xx}	✓		✓	
f_{xxx}	✓	✓	✓	*N1, N2*
f_{xxxx}			✓	

Table 5: The Signs of Derivatives and Parameters

Derivative	Superscript	Difference method	Symbol
f_x	1	Forward	*F*
f_{xx}	2	Backward	*B*
f_{xxx}	3	Central	*C*
f_{xxxx}	4	Others	*N1, N2*

For the part of third order derivative, we have carried out to estimate by adopting the common forward difference method, central difference method and backward difference method, but the excessive computing nodes lead to failed calculation in the code. Although the forward difference method is not affected by the initial boundary points, that the occurrence time of shock wave and contact discontinuity interface are very short but the distance of nodes is big causes huge oscillation problem. It cannot estimate the part of energy ρE even though the consequence of density ρ can be projected. On the operation of initial gradient, therefore, we take the forward difference method for first order derivative, central difference method for second order derivative and compare the results of difference methods *N1* and *N2* for third order derivative.

First, note the density ρ-related graph (as Fig. 1) with considering third order gradient, we debate that it whether improves the catching ability of shock wave and contact discontinuity interface by increasing the accuracy of gradient. By the parts of Fig. 2, we find that the perpendicularity is improved insignificantly although the effect by changing limiter is better than that of this method. In the region between contact discontinuity interface and the front edge of shock wave shown as the Fig. 3, the *N2* method clearly reduces the numerical oscillation problem although the perpendicularity of *N2* method is worse than that of *N1* method. For the *N1* and *N2* method, there are advantages and disadvantages

separately so we further discuss the results of individual energy $\rho_i E_i$.

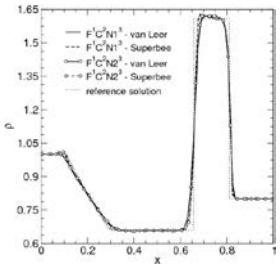

Fig. 1. The ρ -related diagram with considering third order derivative

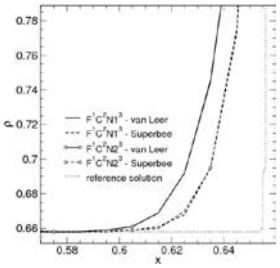

Fig. 2. The enlargement Zoom2 of Fig. 1

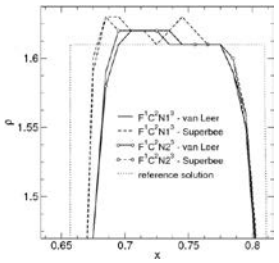

Fig. 3. The enlargement Zoom3 of Fig. 1

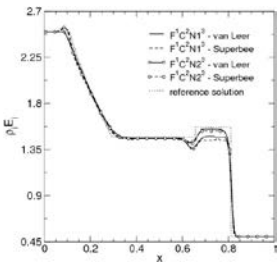

Fig. 4. The ρE -related diagram with considering third order derivative

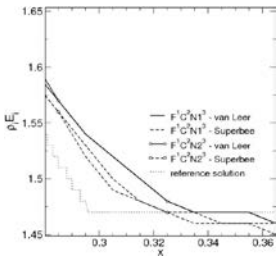

Fig. 5. The enlargement Zoom2 of Fig. 4

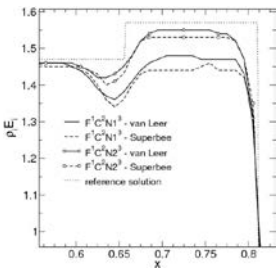

Fig. 6. The enlargement Zoom3 of Fig. 4

For the individual energy $\rho_i E_i$ -related figure (as Fig. 4), we just discussed the results in the regions of the rear of expansion wave and near contact discontinuity interface because other regions are similar to the ρ-related graph and the disparities of these regions are noticeable than that of other regions. By the graph of Zoom 2 (Fig. 5), we know that it can produce the problem of incorrect projection for individual energy after the expansion wave by using the Superbee limiter. We also obtain a consequence that the projection of *N1* is worse than that of *N2*. In addition, by Fig. 6, we observe that using the difference method of *N1* for third-order derivative produces huge oscillations and it has failed projection between contact discontinuity interface and the front edge of shock wave. Moreover, the *N1* method with using the Superbee limiter leads to numerical oscillation problem in this region. Therefore, it is unsuitable that we deal with the discussed flow field problem by applying *N1* method. In order to improve the problem of incorrect estimation for high order derivative, we try to modify the problems of oscillation and faulty projection caused by third order derivative by adding the difference method of adaptive gradient.

Considering the Computing Loop of Adaptive Gradient

In this study, we consider the needed node position of distinct difference types and change the order of computation of gradient difference as Table 4. We try various combinative forms of difference and find that the original failed difference method becomes successful operation as well as improve the difference type of considering third-order gradient through changing the computation way of loop. Additionally, we will list and illustrate the logic of following three sorts of loop design and consequences, including $F^1C^2C^3$, $F^1F^2C^3$ and $F^1C^2N2^3$.

(i) The computation loop of gradient $F^1C^2C^3$:

Although that the central difference method of third order is failure on the computing code was mentioned in the above section, it can operate via modifying the computational loop. In the code, we alter some setting.

(1) If the time stepping $n \le 1$, then we use the first-order forward difference method to estimate the conditional parameter of $n = 2$.
(2) There are some parameters under the condition of time stepping $n = 2$, and then we modify the operation to second-order gradient, where the second order derivative takes central difference method i.e. F^1C^2.
(3) After the above two operations, we change the calculation of gradient into third order and consider the central difference method on the computation of third order derivative. In other words, we start to employ the computing type $F^1C^2C^3$ after $n = 4$.

The computational logic of other two ways is similar to this type, and the illustrations of their computing logic will be simply described as following.

(ii) The computation loop of gradient $F^1C^2F^3$:

(1) If $i = 1$, then ∇f uses the difference operation F^1 of first order gradient.
(2) If $i = 2$, then ∇f uses the difference operation F^1F^2 of second order gradient.
(3) If $i \ge 4$, then ∇f uses the difference operation $F^1F^2C^3$ of third order gradient.

(iii) The computation loop of gradient $F^1C^2N2^3$:

(1) If $i = 1$, then ∇f uses the difference operation F^1 of first order gradient.
(2) If $i = 2$, then ∇f uses the difference operation F^1F^2 of second order gradient.

(3) If $i \geq 4$, then ∇f uses the difference operation $F^1F^2N2^3$ of third order gradient.

We do not consider the forward and backward difference method for third order derivative. The reason is that the needed computing nodes are excessive. For the discussed problem of high gradient on shock wave and contact discontinuity interface, it must lead to a problem of error. Although, for third order derivative, the central difference method needs 5 nodes, it does not cause the failed operation in early stages of computation through the design of loop. In addition, we also adjust the initial position of different order gradient with the difference type.

First, through the density ρ-related graph (Figs. 7 - 9), we observe that the design of computing loop is adapted whether the catching ability of shock wave and contact discontinuity interface rises. In the region between contact discontinuity interface and the front edge of shock wave, we find that the difference method of *N2* with considering Superbee limiter still has a notably numerical oscillation problem. However, the catching ability of perpendicularity of $F^1F^2C^3$ on contact discontinuity interface is better than other two difference methods. Additionally, it improves the numerical oscillations of Superbee limiter in this region. However, it was affected by the characteristic of limit function that the van Leer limiter of smooth type cannot display the contrast significantly between distinct difference methods.

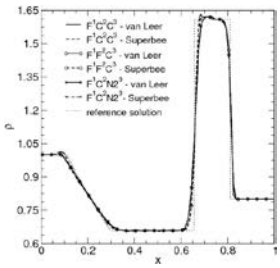

Fig. 7. The ρ-related diagram with computation loop of mixed gradient

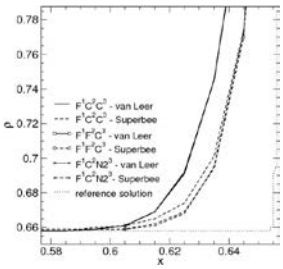

Fig. 8. The enlargement Zoom2 of Fig. 7

Observe the divergences of individual energy $\rho_i E_i$ (Fig. 10), by the graph of Zoom2 (as Fig. 11), we can notice that the approximation effect in the rear edge of expansion wave is the best by using the difference method $F^1F^2C^3$. Nevertheless, it still cannot improve the problem of numerical error of energy ρE before the contact discontinuity interface even through modifying the loop of calculation. Note the figure of Zoom 4 (as Fig. 12), we can clearly perceive that the disparity between these three difference methods with various limiters. In the above section, the best difference method $F^1C^2N2^3$ of third order derivative has no capability to project the numerical values of energy in the region between contact discontinuity interface and the front edge of shock wave. Thus, through modifying the loop of computation, the oscillation problem also cannot be improved in the front of contact discontinuity interface. Hence, in this region, the error of energy estimation is pretty outstanding. Oppositely, the results of original other difference methods are better than that of $F^1C^2N2^3$ clearly in this region.

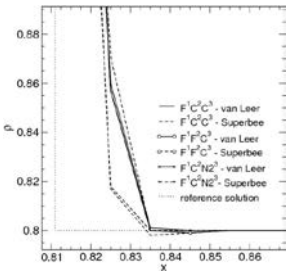

Fig. 9. The enlargement Zoom4 of Fig. 7

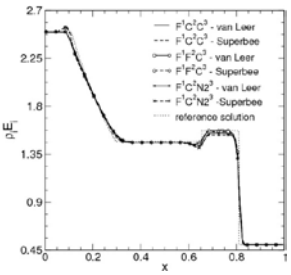

Fig. 10. The ρE-related diagram with computation loop of mixed gradient

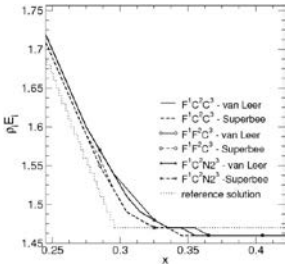

Fig.11. The enlargement Zoom2 of Fig. 10

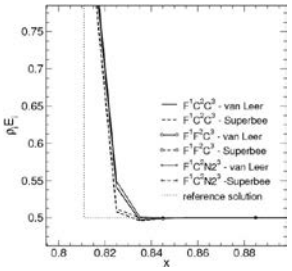

Fig.12. The enlargement Zoom4 of Fig. 10

It is worth noting that the numerical method with van Leer limiter can correctly project the estimation of energy in this region. Although there is a problem of numerical oscillation, the gradient operation extends to the accuracy of third order and has appropriate reliability through this modificatory method of loop. By the above section, we will discuss and integrate the results of better difference method of gradient operation.

Comparison of Difference Method with Distinct Order and Mixture Gradient

By the above optimal computation results, we debate the influence of computing code including the additional energy term with using variant order difference methods. The content contains the first order gradient F^1, second order gradient F^1C^2 and third order gradient $F^1F^2C^3$ with single gas condition as well as van Leer and Superbee limiter.

For the ρ-related part as Figs. 13 - 15, we just detail the numerical oscillation problem in the regions of the front edge of expansion wave and between shock and contact discontinuity interface because the dissimilarities are fewer on the contact discontinuity interface and the rear edge of shock wave. By the front edge of expansion wave, we find that the consequences of second order gradient F^1C^2 and third order gradient $F^1F^2C^3$ with using Superbee limiter decrease the problem of numerical oscillation

slightly, although the estimation of expansion wave oppositely deviates the curve of the reference solution because of the immense slope. However, considering van Leer limiter, the estimation of second order gradient is better than other two types of difference method. In the region between shock and contact discontinuity interface, the difference type with high order has the numerical oscillation problem. Especially, for applying Superbee limiter, the difference method with second order accuracy causes the most oscillations.

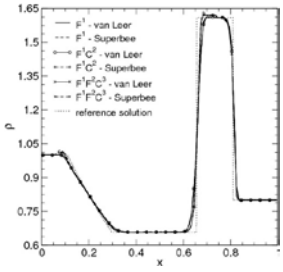

Fig. 13. The ρ -related diagram with distinct order difference types

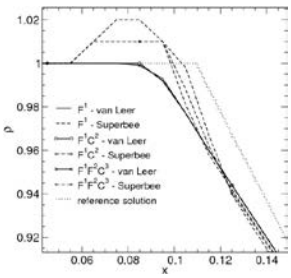

Fig. 14. The enlargement Zoom1 of Fig. 13

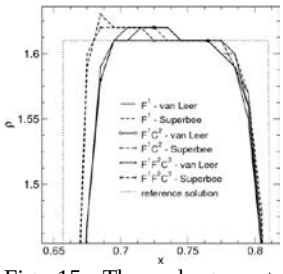

Fig. 15. The enlargement Zoom3 of Fig. 13

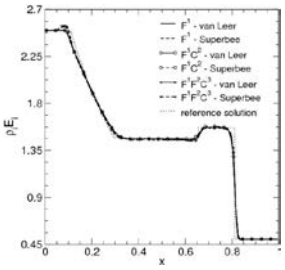

Fig. 16. The $\rho_i E_i$ -related diagram with distinct order difference types

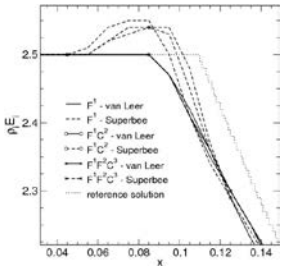

Fig. 17. The enlargement Zoom1 of Fig. 16

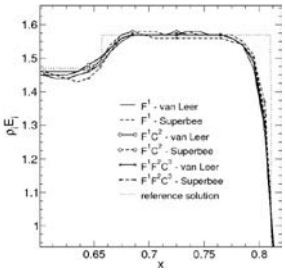

Fig. 18. The enlargement Zoom3 of Fig. 16

For the individual energy $\rho_i E_i$ -related figure as Fig. 16, on the front edge of expansion wave, the oscillation position of the difference method with using Superbee limiter moves onward with the increasing order. In other words, in this region, enlarging the order can improve the calculation accuracy of catching expansion wave and reduce the strength of oscillation. In addition, the projection capability of energy is the best through the gradient calculation F^1C^2 of second order accuracy in the regions where are the front edge of contact discontinuity interface and between the front edge of shock and contact discontinuity interface. However, augmenting the order and the problem of computing nodes will result in plenty of numerical oscillations. After the modification of the loop, as Zoom3 (Fig. 18) there is an apparent dissimilarity on the forecast of energy.

Through this series of related diagram, for the gradient calculation of additional energy equation of multiple gases, the perpendicularity of Superbee limiter are better than that of van Leer limiter on the non-linear region, although the problems of numerical oscillation and inaccurate forecast are quite grave. By this section, we know that using the gradient computation method of second order accuracy will match the characteristic of fast variation of shock due to less computing nodes and improve the computation precision and non-physical numerical oscillations.

The Numerical Results in Different Type for Gradient

The following adopted difference methods are forward and central difference method, and the chosen flux limiters are van Leer, Superbee as well as the compressive form of Čada limiter.

a. Comparison between the results of $F^1C^2C^3$ and the one of $F^1C^2C^3C^4$

First, we discuss the consequence of the fourth-order and third-order Taylor series for the 1-dimensional gradient in this part. For the density ρ-related diagram Fig. 19, we directly observe the enlargement figure in the region before the contact discontinuity interface showed as Fig. 21. We find that the perpendicularity of the fourth-order series is not manifestly better than the one of third-order series. However, the numerical oscillations of the fourth-order series explicitly become more serious. For the region of expansion wave in Fig. 19, the numerical results of the Superbee limiter and van Leer limiter are rough, but that of Čada limiter comparatively approximates the reference solution. Besides, in the location between the contact discontinuity interface and shock wave as Fig. 22, the fourth-order result is also worse compared with the result of third-order. Nevertheless in the Fig. 20, there is almost no conspicuous difference.

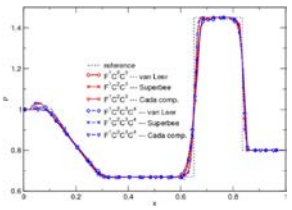

Fig. 19. The ρ -related diagram with the different order derivative

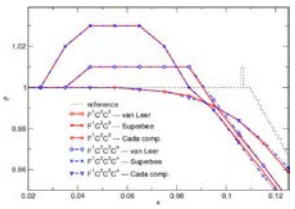

Fig. 20. The enlargement of Fig. 19 near the expansion wave

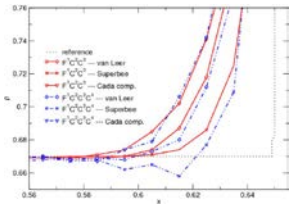

Fig. 21. The enlargement of Fig. 19 near the contact discontinuity interface

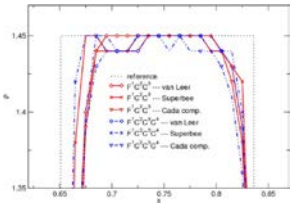

Fig. 22. The enlargement of Fig. 19 between the contact discontinuity interface and shock wave

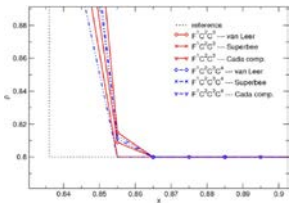

Fig. 23. The enlargement of Fig. 19 near the shock wave

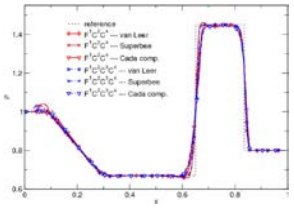

Fig. 24. The ρ -related diagram with considering whether there is the 3^{rd} order for the gradient treatment

b. Comparison between the results of $F^1C^2C^4$ and the one of $F^1C^2C^3C^4$

Here, for the gradient calculation by expanding Taylor series into fourth order, we debate whether the numerical oscillations before the high-gradient position can be improving through removing the third-order part. As the density ρ-related Fig. 24, we discuss the above problem. In the Fig. 25, their tendencies are similar to the above part a. In addition, we find that there is almost no the difference for the perpendicularity capturing in the local enlargement diagrams Fig. 26 and Fig. 27; however, the non-physical numerical oscillations of the form of removing the third-order derivative become serious.

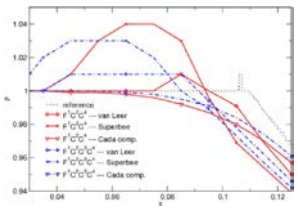

Fig. 25. Local position diagram of Fig. 24

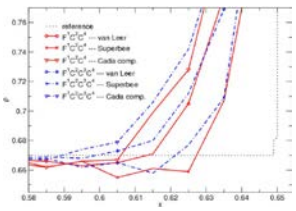

Fig. 26. Local position diagram of Fig. 24

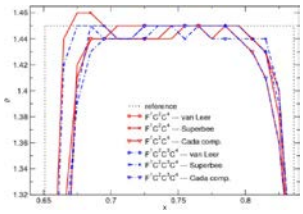

Fig. 27. Local position diagram of Fig. 24 between the contact discontinuity interface and shock wave

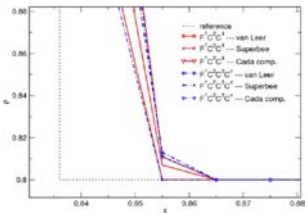

Fig. 28. Local position diagram of Fig. 24 near the shock wave

Furthermore, the numerical oscillations of adopting the different limiters have discrepancies. In Fig. 26, the oscillation phenomena will be improved via the numerical computation combining with the compressive-form Čada limiter. Hence, we think that the facing oscillation problem can be improved through some high-order numerical method with a fit limiter.

CONCLUSIONS

In order to reduce the non-physical oscillation problem in the numerical process, in this study, we carried out several newly derived gradient difference method as well as different two kinds of flux limiter to modify the form of the high-order Taylor series in source term for multispecies.

The results present that the nodes of difference are excessive will cause the numerical oscillation problem and failed computation because the high gradient varies sharply. Therefore, for the gradient computing, we raise the computing precision of gradient difference method by modifying computation loop. For the presented results of **part a**, the perpendicularity of the fourth-order series is not manifestly better than that of third-order series, but the non-physical numerical oscillations of the fourth-order series definitely become more serious. Moreover, the numerical result of Čada limiter closer the reference solution than that of Superbee/van Leer limiter. Further, in the **part b**, the non-physical numerical oscillations become aggravated for the form of removing the third-order derivative. The oscillation phenomen could be improved through some high-order numerical computation combining with a fit limiter.

ACKNOWLEDGMENTS

This study was supported by the Ministry of Science and Technology (MOST107-2221-E-035-043-MY2 & MOST104-2221-E-035-052- & MOST103-2632-E -035-001-MY3 & MOST103-2221-E -35-064-) as well as Zonta International (Amelia Earhart Fellowship), we want to thank for the valuable help cordially. And we are kindly grateful to Ms. Min-Chun Chen for her assistance in this study.

REFERENCES

Čada, M., "Compact third-order limiter functions for finite volume methods." Dipl. Geo Physiker, Ludwig-Maximilians University. (2009)

Godunov, S.K., "A difference method for numerical calculation of discontinuous equation of hydrodynamics." Math Sbornik (in Russian) 47: 217-306. (1959).

Jameson, A., Schmidt, W. and Turkel, E., "Numerical solutions of the Euler equations by finite volume methods using Runge-Kutta time-stepping schemes." AIAA paper:

1981-1259. (1981).
Liou, M.S. and Steffen, C.J., "A flux splitting scheme." NASA TM104404, (1991); Journal of Computational Physics 107: 23-39. (1996).
Shieh, T.H. and Li, M.R., "Numeric treatment of contact discontinuity with multi gases." Journal of Computational and Applied Mathematics 230 (2): 656-673. (2009).
Ton, V.T., "Improved shock-capturing methods for multicomponent and reacting flows." Journal of Computational Physics 128: 237-235. (1996).
van Leer, B., "On the relation between the upwind-differencing schemes of Godunov, Engquist-Osher and Roe." Journal on Scientific and Statistical Computing 5: 1-20. (1984).
van Leer, B., "Upwind and high-resolution methods for compressible flow: From donor cell to residual-distribution schemes." Communications in Computational Physics 1 (2):192-206. (2006).
Wada, Y. and Liou, M. S., "A flux splitting scheme with high-resolution and robustness for discontinuities." AIAA-94-0083 (1994).
Xu, K. and Prendergast, K.H., "Numerical Navier-Stokes solutions from gas kinetic theory." Journal of Computational Physics 114: 9-17. (1994)

NOMENCLATURE

Greek Symbol

Symbol	Illustration	Units
Δ	Difference	[–]
ϕ	Conservation variables $\phi = \Delta x U'_K$	$[N/m^2]$
Φ	Flux function	$[N/m^2]$
γ	Ratio of specific heats	[–]
φ	Limit function	[–]
ν	Courant number $\upsilon = v_{\max}\,\Delta t/\Delta x$	[–]
ρ	Density	$[kg/m^3]$
ς	Specific volume $\varsigma = 1/\rho$	$[m^3/kg]$

Latin Symbol

Symbol	Illustration	Units
C_{CFL}	CFL number $\Delta t = (\Delta x/v_{\max})C_{CFL}$	[–]
e	Specific internal energy	$[J/kg]$
E	Specific energy	$[J/kg]$
F	Frictionless flux vector	$[N/m^2]$
h	Entropy	$[kJ/kg]$
P	Pressure	$[psi]$
Q	Source term	$[N/m^2]$
r	Specific local flux	[–]
R	Gas constant	$[J/kg\cdot K]$
s	Switching function	[–]
t	Time	[sec]
T	Temperature	$[K]$
u	Velocity in x-axis	$[m/s]$
U	Vector of conservation variables	$[N/m^2]$
$v_{\max}$	Maximum propagation velocity	$[m/s]$
V	Volume	$[m^3]$
∂V	Unit surface	$[m^2]$
W_i	Molar mass	$[kg/kmol]$
Y_i	Mass fraction $Y_i = \rho_i/\rho$	[–]

Mathematical Symbol

Symbol	Illustration	Units
$\overline{U}$	Mean value of conserved variable vector	[–]
max	Maximum	[–]
min	Minimum	[–]

Index Symbol

Symbol	Illustration	Units
i, j	Step number of individual displacement	[–]
K	Individual control volume	$[m^3]$
s	Average	[–]

新差分法對源項參數梯度問題的數值處理

謝宗翰　　李明融　　李育佐　　陳勇廷

逢甲大學航太與系統工程學系
逢甲大學機械與航空工程博士學位學程
國立政治大學應用數學系
明新科技大學機械工程系

摘 要

本文將非定常 Euler 方程之能量方程擴展為混合氣體的形式，並透過有限體積法進行數值求解，進而討論接觸不連續界面和震波附近之非物理性數值振盪問題。我們透過使用結合不同通量限制器的 AUSMDV 黎曼求解法，利用有限體積法以及二階二步時間離散步進法來求解方程。接著，本文為了討論近似黎曼求解法在不同類型梯度數值處理中所面臨的問題，透過建立新的梯度控制方法來檢驗非物理性數值振盪問題。